

Available online at www.sciencedirect.com

ScienceDirect

www.elsevier.com/locate/jes

Chemical characteristics of fine particles and their impact on visibility impairment in Shanghai based on a 1-year period observation

Min Zhou^{1,2}, Liping Qiao^{1,2}, Shuhui Zhu^{1,2}, Li Li^{1,2,*}, Shengrong Lou^{1,2}, Hongli Wang^{1,2}, Qian Wang^{1,2}, Shikang Tao^{1,2}, Cheng Huang^{1,2}, Changhong Chen^{1,2}

1. State Environmental Protection Key Laboratory of the Cause and Prevention of Urban Air Pollution Complex, Shanghai 200233, China.

E-mail: zhoum@saes.sh.cn

2. Shanghai Academy of Environmental Sciences, Shanghai 200233, China

ARTICLE INFO

Article history:

Received 26 October 2015

Revised 9 January 2016

Accepted 25 January 2016

Available online 5 April 2016

Keywords:

PM_{2.5}

Chemical composition

Light extinction efficient

Shanghai

ABSTRACT

In this work, a one-year observation focusing on high time resolution characteristics of components in fine particles was conducted at an urban site in Shanghai. Contributions of different components on visibility impairment were also studied. Our research indicates that the major components of PM_{2.5} in Shanghai are water-soluble inorganic ions and carbonaceous aerosol, accounting for about 60% and 30% respectively. Higher concentrations of sulfate (SO₄²⁻) and organic carbon (OC) in PM_{2.5} occurred in fall and summer, while higher concentrations of nitrate (NO₃) were observed in winter and spring. The mass concentrations of Cl⁻ and K⁺ were higher in winter. Moreover, NO₃ increased significantly during PM_{2.5} pollution episodes. The high values observed for the sulfate oxidizing rate (SOR), nitrate oxidizing rate (NOR) and secondary organic carbon (SOC) in OC indicate that photochemical reactions were quite active in Shanghai. The IMPROVE (Interagency Monitoring of Protected Visual Environments) formula was used in this study to investigate the contributions of individual PM_{2.5} chemical components to the light extinction efficient in Shanghai. Both NH₄NO₃ and (NH₄)₂SO₄ had close relationships with visibility impairment in Shanghai. Our results show that the reduction of anthropogenic SO₂, NO_x and NH₃ would have a significant effect on the improvement of air quality and visibility in Shanghai.

© 2016 The Research Center for Eco-Environmental Sciences, Chinese Academy of Sciences.

Published by Elsevier B.V.

Introduction

Particulate matter plays an important role in the atmosphere, affecting the Earth's climate system by absorbing and scattering solar radiation. Because of its impact on atmospheric visibility and human health, fine particulate matter has attracted more and more concern in recent years (Huang et al., 2014; Jung et al., 2009; Sokolik & Toon, 1996; Qiao et al., 2014).

The chemical composition of fine particulate matter is quite complicated, including primary particulate matter, secondary inorganic ions (SO₄²⁻, NO₃, NH₄⁺), carbon aerosol (EC (elemental carbon), OC (organic carbon)), crustal elements and water (Seinfeld & Pandis, 2006; Sun et al., 2014). Different compositions have different impacts on the light extinction coefficient, cloud formation process, climate system and human health (Li et al., 2015; Kulkarni et al., 2015; Quan et al., 2014). Therefore, to study the chemical characteristics of

* Corresponding author. E-mail: lili@saes.sh.cn (Li Li).

the fine particulate matter is of great significance, and is helpful in explaining the pollution sources, formation mechanism, migration, biological effects and effect on human health of particulate matter (Tang et al., 2006; Tao et al., 2014; Pateraki et al., 2014). Many works have been reported in this field. Zhang et al. (2013) studied the seasonal characteristics of water-soluble ions, OC, EC and elements in PM_{2.5} in Beijing. They showed that different meteorological and synoptic conditions could change the chemical composition of the particle distribution, and obtained six major sources of PM_{2.5} by using the PMF model. There is also research investigating the characteristics of organic carbon and elemental carbon in PM_{2.5} in California, Pennsylvania and Xian, which estimates the concentrations of secondary organic carbon using the EC-tracer method and Chemical Mass Balance receptor model (Na et al., 2004; Cabada et al., 2004; Cao et al., 2005). Sun et al. (2006) and Wang et al. (2006b) investigated the particulate matter mass concentrations, water-soluble ions and carbon aerosol under different pollution episodes including dust, haze, and clear days, and established the different formation mechanisms by combining the climate conditions and anthropogenic pollution sources. Huang et al. (2012) provided a complementary picture of typical haze types and the formation mechanisms in megacities over China by using a synergy of ground-based monitoring, satellite and lidar observations. Liu et al. (2013) found that the key factors affecting the formation and evolution of a regional haze episode were stable anti-cyclone synoptic conditions at the surface layer, decrease of the planetary boundary layer (PBL) height, heavy pollution emissions from urban areas, number and size evolution of aerosols, and hygroscopic growth for aerosol scattering. Han et al. (2015) found that the proportional contributions of ammonium sulfate and ammonium nitrate to light extinction were higher during hazy times than during non-hazy days. However, available studies on particulate matter have focused on the chemical characteristics of fine particles and their impact on visibility impairment based on off-line data, and there is a lack of direct observation evidence showing the impact from chemical species at high time resolution for a long period.

Shanghai, one of the largest commercial and industrial cities in China, continually suffers from severe and complex air pollution. The atmospheric haze phenomenon caused by high particle mass concentrations, which greatly decreases the visibility, is very common in Shanghai (Fu et al., 2008; Huang et al., 2012; Wang et al., 2012). In this study, we have performed a one-year continuous PM_{2.5} sampling campaign at an urban site in Shanghai and focused the study on the seasonal variations of chemical compounds identified by on-line instruments. The analysis focuses on the following issues: (1) annual variations of particulate matter and major chemical compounds in PM_{2.5} in Shanghai; (2) ambient concentration levels of different chemical components and their seasonal variations; (3) proportions of chemical components of PM_{2.5} during different pollution episodes; (4) characterization of secondary components in PM_{2.5} in Shanghai; (5) contributions of chemical components in PM_{2.5} on visibility impairment. The results are very important for understanding the pollution characteristics and potential sources, and also of great importance for policy makers to improve the air quality.

1. Materials and methods

1.1. Sampling sites and descriptions

The observational site in this study is located in Shanghai Academy of Environmental Sciences (SAES, 31°10'N, 121°25'E), which is in the southwest of Shanghai, in a commercial and residential mixed district. The sampling height was at 15 m above the ground level. About 500 m east from this sampling site is the Humin Traffic Road, 150 m south is the Caobao Road. There is no significant industrial source around this sampling site, which could be regarded as a representative urban area in Shanghai.

1.2. Sample collection and analysis

The observational period was from January 1st to December 31st, 2011. The mass concentrations of PM₁₀, PM_{2.5} and PM_{1.0} were simultaneously measured by an on-line PM monitor (FH 62 C14 series, Thermo Fisher Scientific) using beta attenuation techniques operated at a flow rate of 16.67 L/min. The detection limit was below 1 µg/m³, and the time resolution was 5 min.

An on-line analyzer for monitoring aerosols and gases (MARGA ADI 2080, Applikon Analytical B.V) (Du et al., 2011) through a PM_{2.5} cyclone was applied to measure the mass concentrations of major water-soluble inorganic ions (Cl⁻, NO₃⁻, SO₄²⁻, NH₄⁺, Na⁺, K⁺, Ca²⁺, Mg²⁺) in PM_{2.5} at one hour resolution, and the detection limits for all components were 0.1 µg/m³, except for K⁺ (0.16 µg/m³), Mg²⁺ (0.12 µg/m³) and Ca²⁺ (0.12 µg/m³). The air sample was drawn through a wet rotating annular denuder (WRD) where water-soluble gases diffused into the absorption solution (0.0035% H₂O₂), then particles were collected in a stream-jet aerosol collector (SJAC). The absorption solutions were drawn from the WRD and the SJAC using syringes and subsequently injected into ion chromatographs with an internal standard (LiBr) for component analysis once every hour (Qiao et al., 2014; Du et al., 2010).

A Thermal/Optical Carbon Aerosol Analyzer (model RT-4, Sunset laboratory Inc.) operated with a thermal/optical transmittance principle was used for the carbon analysis. It was equipped with a PM_{2.5} cyclone and an upstream parallel-plate organic denuder. OC and EC in PM_{2.5} were analyzed at a flow rate of 8 L/min with a two-stage thermal procedure (600–840°C in a He atmosphere and 550–650–870°C in an oxidizing atmosphere of 2% O₂ with He as diluent gas). The detection limit was 0.5 µg/m³, and the time resolution was 1 hr for each sample, with 45 min of sampling and 15 min of analysis.

Trace gases including ozone (O₃), sulfur dioxide (SO₂) and nitrogen oxides (NO_x) were evaluated. O₃ was measured by an O₃ monitor (Model EC9811, Ecotech Inc) at 5 min time resolution; the detection limit was 0.5 ppbv. SO₂ was measured by a SO₂ monitor (Model EC9580B, Ecotech Inc) at 5 min resolution; the detection limit was 0.5 ppbv. NO_x was measured by a NO_x monitor (Model 42i, Thermo Fisher Scientific Inc) at 5 min resolution, and the detection limit was 0.5 ppbv. The relative humidity (RH) and visibility were also measured at 1 hr time resolution in this station.

2. Results

2.1. Particulate matter pollution characteristics in urban Shanghai area

The time series of the airborne particulate matter concentrations from January 1st to December 31st in 2011 is shown in Fig. 1. As shown from the figure, the average mass concentrations of PM_{10} , $PM_{2.5}$, and $PM_{1.0}$ were (88 ± 66) , (49 ± 47) and $(35 \pm 30) \mu\text{g}/\text{m}^3$, respectively. The ratios of $PM_{1.0}/PM_{2.5}$, $PM_{1.0}/PM_{10}$ and $PM_{2.5}/PM_{10}$ were 71.4%, 39.7% and 55.6%, respectively, indicating that fine particles dominated PM_{10} . In 2011, the annual average concentration of atmospheric $PM_{2.5}$ in Shanghai was lower than the reported value of $94.6 \mu\text{g}/\text{m}^3$ measured from September 2003 to January 2005 (Wang et al., 2006a), and $57.9 \mu\text{g}/\text{m}^3$ and $61.4 \mu\text{g}/\text{m}^3$ at two sites in Shanghai, respectively, measured from 1999 to 2000 (Ye et al., 2003). This shows that the air quality of Shanghai in 2011 was relatively better than in previous years.

As shown in Fig. 1, the PM concentrations in summer were relatively lower than in other seasons. The heaviest particulate matter pollution episode occurred in early May, when the maximum hourly concentrations of PM_{10} and $PM_{2.5}$ reached 999 and $185 \mu\text{g}/\text{m}^3$, respectively. This episode was mainly due to intrusion of a dust storm in northwest China (Li et al., 2014). The highest monthly average concentration of PM_{10} occurred in May, which was $148 \pm 177 \mu\text{g}/\text{m}^3$; while the lowest was in August, with the average concentration of $49 \pm 26 \mu\text{g}/\text{m}^3$. The

high concentration that occurred in May was due to coarse particulate pollution that emerged after sand and dust weather. However, the more favorable diffusion conditions in summer made it difficult for pollutant accumulation, causing low particulate matter concentrations during August and September. For $PM_{2.5}$, the highest monthly-average concentration, $74 \pm 70 \mu\text{g}/\text{m}^3$, occurred in February; while the lowest, $31 \pm 18 \mu\text{g}/\text{m}^3$, occurred in September. The high precursor emissions accompanied by worse diffusion conditions in winter were the reasons for the frequent appearance of high concentrations of fine particles (Park et al., 2004).

2.2. Chemical composition characterization of $PM_{2.5}$ in urban Shanghai area

2.2.1. Seasonal characteristics of chemical components in $PM_{2.5}$
Fig. 2 and Table 1 show the seasonal concentrations of water-soluble inorganic ions, organic matters (OM = OC \times 1.4) (Turpin et al., 2001) and EC in $PM_{2.5}$ in urban Shanghai in 2011.

Among all the seasons in 2011, winter had the most serious pollution. The mass concentration of $PM_{2.5}$ arranged from high to low follows the order winter, spring, fall, summer. Among the chemical components of $PM_{2.5}$, secondary inorganic ions including NO_3^- , SO_4^{2-} , NH_4^+ and organic matter (OM) constituted the largest proportion, accounting for 75.2%–94.0% in total. In comparison, the proportion of Cl^- , Mg^{2+} , K^+ , Ca^{2+} , and Na^+ was low. The $PM_{2.5}$ chemical composition changed with the seasons, and had a close relationship with weather

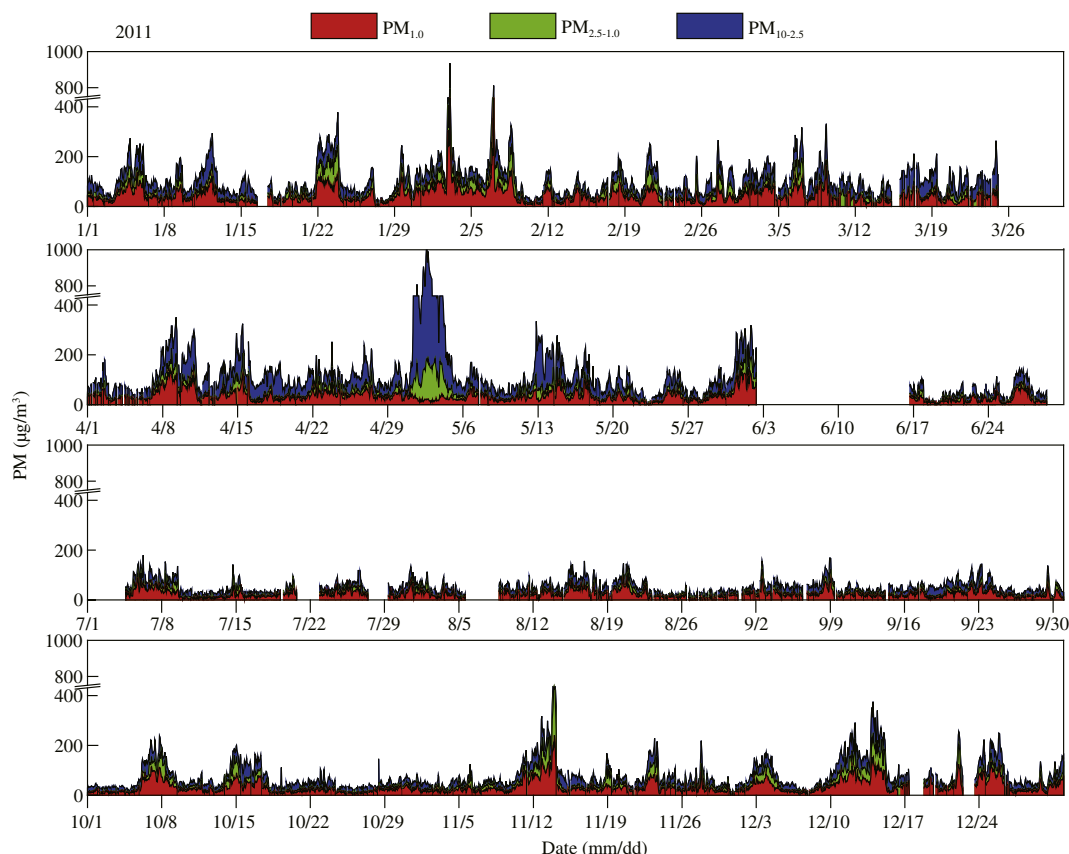


Fig. 1 – Time series of the particulate matter mass concentrations in Shanghai in 2011.

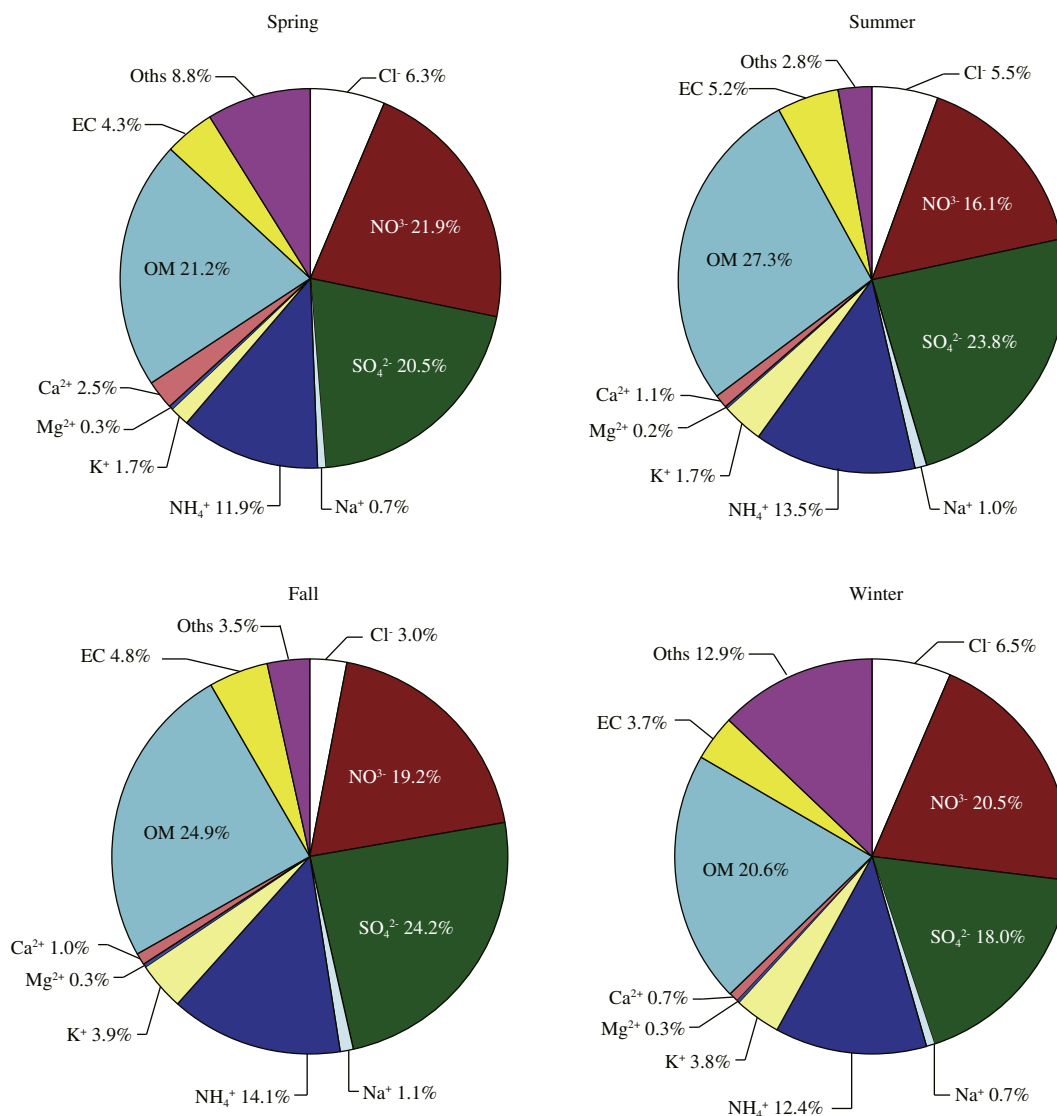


Fig. 2 – Seasonal change of PM_{2.5} chemical components in Shanghai in 2011.

Table 1 – Concentrations of PM₁₀, PM_{2.5} and the components of PM_{2.5} in various seasons in 2011.

Periods	Spring	Summer	Fall	Winter
	Mar–May	Jun–Aug	Sep–Nov	Jan–Feb, Dec
PM _{2.5}	55 ± 35	34 ± 26	40 ± 39	65 ± 55
PM ₁₀	122 ± 114	55 ± 38	64 ± 50	101 ± 73
Cl ⁻	3.50 ± 1.60	2.21 ± 1.20	1.20 ± 1.28	4.21 ± 6.21
NO ₃ ⁻	12.07 ± 9.93	6.43 ± 7.58	7.67 ± 10.66	13.33 ± 11.23
SO ₄ ²⁻	11.29 ± 7.71	9.54 ± 6.99	9.67 ± 8.78	11.70 ± 10.16
Na ⁺	0.36 ± 0.22	0.39 ± 0.23	0.42 ± 0.20	0.43 ± 0.18
NH ₄ ⁺	6.53 ± 5.73	5.41 ± 4.75	5.62 ± 6.26	8.11 ± 6.05
K ⁺	0.92 ± 0.99	1.39 ± 1.20	1.57 ± 0.91	2.46 ± 8.03
Mg ²⁺	0.19 ± 0.16	0.08 ± 0.06	0.11 ± 0.06	0.17 ± 0.34
Ca ²⁺	1.36 ± 1.09	0.45 ± 0.25	0.39 ± 0.19	0.48 ± 0.28
TWSII	35.95 ± 23.17	25.78 ± 19.38	26.42 ± 26.33	40.73 ± 34.41
SNA	29.79 ± 22.23	21.37 ± 18.09	22.97 ± 24.93	33.14 ± 25.73
OC	9.72 ± 4.95	9.10 ± 6.51	8.27 ± 6.95	11.18 ± 7.24
EC	2.35 ± 1.64	2.06 ± 1.52	1.93 ± 1.56	2.43 ± 2.01

conditions (the PBL height, temperature, relative humidity, diffusion conditions, etc.) and precursor emissions. These factors determined particulate formation, growth, transformation and aging processes (Hu et al., 2009). The total mass concentrations of water-soluble inorganic ions (TWSII) and that of SO₄²⁻, NO₃⁻, NH₄⁺ (SNA) in PM_{2.5} in spring were (35.95 ± 23.17) and (29.79 ± 22.23) μg/m³, respectively. TWSII and SNA accounted for 65.4% and 54.2% of PM_{2.5}, respectively. The mass concentrations of chemical components arranged from high to low were NO₃⁻ > SO₄²⁻ > OC > NH₄⁺ > Cl⁻ > EC > Ca²⁺ > K⁺ > Na⁺ > Mg²⁺. PM pollution occurred frequently in spring and the secondary generation of NO_x was significant. The mass concentrations of TWSII and SNA in PM_{2.5} in summer were (25.78 ± 19.38) and (21.37 ± 18.09) μg/m³, respectively. TWSII and SNA accounted for 75.8% and 62.9% in PM_{2.5}, respectively. The mass concentrations of chemical components arranged from high to low were SO₄²⁻ > OC > NO₃⁻ > NH₄⁺ > Cl⁻ > EC > K⁺ > Ca²⁺ > Na⁺ > Mg²⁺. The strong sunlight

in summer contributed to the formation of secondary organic carbon and accelerated the transformation of volatile components (NO_3 , NH_4^+ , etc.) from the particulate phase to the gaseous phase. The mass concentrations of TWSII and SNA in $\text{PM}_{2.5}$ in fall were (26.42 ± 26.33) and (22.97 ± 24.93) $\mu\text{g}/\text{m}^3$, respectively, accounting for 66.1% and 57.4% in $\text{PM}_{2.5}$, respectively. The mass concentrations of chemical components arranged from high to low were $\text{SO}_4^{2-} > \text{OC} > \text{NO}_3^- > \text{NH}_4^+ > \text{EC} > \text{Cl}^- > \text{K}^+ > \text{Ca}^{2+} > \text{Na}^+ > \text{Mg}^{2+}$, which matches the results in summer showing that higher concentrations of SO_4^{2-} and OC existed in $\text{PM}_{2.5}$. In winter, the mass concentrations of TWSII and SNA in $\text{PM}_{2.5}$ were (40.73 ± 34.41) and (33.14 ± 25.73) $\mu\text{g}/\text{m}^3$, respectively. Their proportions in $\text{PM}_{2.5}$ were 62.7% and 51.0%, respectively. The mass concentrations of chemical components from high to low were $\text{NO}_3^- > \text{SO}_4^{2-} > \text{OC} > \text{NH}_4^+ > \text{Cl}^- > \text{K}^+ > \text{EC} > \text{Ca}^{2+} > \text{Na}^+ > \text{Mg}^{2+}$, which matches the results in spring showing that a high concentration of NO_3^- was contained in $\text{PM}_{2.5}$. The difference between winter and other seasons was that winter had higher concentrations of Cl^- and K^+ , probably due to the large numbers of combustion activities taking place (Safai et al., 2010; Park et al., 2004).

From the results above, we can see that for all seasons in 2011, total water-soluble ions in $\text{PM}_{2.5}$ accounted for over 60% of the mass concentration of fine particles and carbonaceous species accounted for about 30%, which illustrates the serious inorganic and organic pollution in Shanghai (Hu et al., 2009). The mass concentration of three secondary inorganic ions (SNA, SO_4^{2-} , NO_3^- , NH_4^+) accounted for about 55% of fine particles, and all OC/EC ratios were more than 4, indicating that secondary pollution formation was very serious and photochemical reactions were active. Primary ions like Mg^{2+} , K^+ , Ca^{2+} , and Na^+ had a relatively lower proportion in fine particles, and their seasonal change was much smaller. However, due to the dust weather from northern China in spring, the proportion of soil components like Ca^{2+} and Mg^{2+} in WSII in Shanghai increased slightly, compared with other seasons, and a similar result was also found in other studies (Wang et al., 2005, 2006b).

2.2.2. Chemical components of $\text{PM}_{2.5}$ in different $\text{PM}_{2.5}$ pollution level days

Investigating the mass concentrations of particles with different sizes and their chemical components can help provide a better understanding of the aging characteristics and chemical processing of particles.

Fig. 3 shows the chemical components of $\text{PM}_{2.5}$ for various $\text{PM}_{2.5}$ concentrations observed in 2011. From this figure, we can find that when the $\text{PM}_{2.5}$ concentration was lower than $20 \mu\text{g}/\text{m}^3$, primary ions (Cl^- , K^+ , Ca^{2+} , Mg^{2+} and Na^+) accounted for 15.3%–28.7% in total in all components, secondary inorganic ions (SO_4^{2-} , NO_3^- and NH_4^+) accounted for 30.4%–49.3%, and OM and EC accounted for 34.1%–48.7%. With the increase of particulate mass concentration, the proportion of primary inorganic ions decreased, accounting for 15.1%–4.9%. On the contrary, the proportion of SNA rose continuously, up to 81.6%, showing the particulate aging process. The longer the particulate aging process, the higher the proportion of SO_4^{2-} , NO_3^- and NH_4^+ in $\text{PM}_{2.5}$ (Moffet et al., 2008). However, from Fig. 3 it can be found that the proportion of SO_4^{2-} , which accounted for $(22.0 \pm 2.4)\%$ in all components, changed very little with

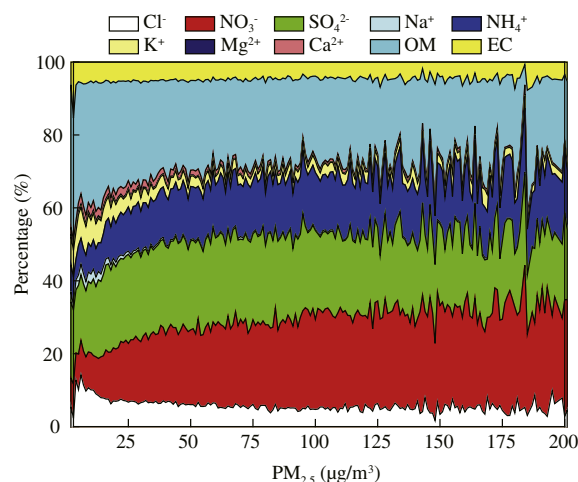


Fig. 3 – Chemical composition of $\text{PM}_{2.5}$ under different concentrations in Shanghai in 2011.

the increase of $\text{PM}_{2.5}$ mass concentration, while the proportion of NH_4^+ and NO_3^- increased significantly. This result shows that NH_4^+ and NO_3^- played an important role in the particulate aging process.

To verify this result, the chemical composition distributions of $\text{PM}_{2.5}$ on different types of pollution days were studied. Fig. 4 shows the proportions of chemical components of $\text{PM}_{2.5}$ on days with different $\text{PM}_{2.5}$ pollution levels. The level air quality is defined into three categories according to the Chinese National Ambient Air Quality (GB 3095–2012) standard: “clean” for days meeting the first grade of NAAQS, “slight pollution” for days meeting the second grade of NAAQS, and “heavy pollution” for days exceeding the second grade of NAAQS. On clean days, OM dominated the $\text{PM}_{2.5}$ mass concentration (28.5%), followed by SO_4^{2-} (22.7%), NO_3^- (15.5%), NH_4^+ (11.1%) and Cl^- (7.2%). OM still accounted for the largest proportion of $\text{PM}_{2.5}$ on slight pollution days, but NO_3^- and NH_4^+ fractions increased significantly. For example, NO_3^- increased from 15.5% to 19.9%, and NH_4^+ increased from 11.1% to 13.5%. NO_3^- had the largest proportions on heavy pollution days, and increased from 15.5% on clean days to 21.0% on heavy pollution days. OM, SO_4^{2-} and NH_4^+ contributed 18.8%, 18.2% and 12.6% to $\text{PM}_{2.5}$, respectively. In addition, the undetected component proportion increased with the deterioration of particulate pollution status, while the OM and EC proportion decreased. The mass concentrations and proportions of NO_3^- and undetected components prominently increased with the aggravation of particulate pollution, similar to the above result. With the exacerbation of $\text{PM}_{2.5}$ pollution, the concentrations of OM, EC, Cl^- , Ca^{2+} , Mg^{2+} and Na^+ increased, but their proportions in $\text{PM}_{2.5}$ decreased. This analysis suggests that NO_3^- was the most important chemical component and increased significantly during heavy $\text{PM}_{2.5}$ pollution days.

2.3. Characteristics of the secondary aerosol in $\text{PM}_{2.5}$

2.3.1. SO_4^{2-} and NO_3^-

SO_4^{2-} and NO_3^- are important chemical components in $\text{PM}_{2.5}$, accounting for about 40% of total $\text{PM}_{2.5}$. They are formed

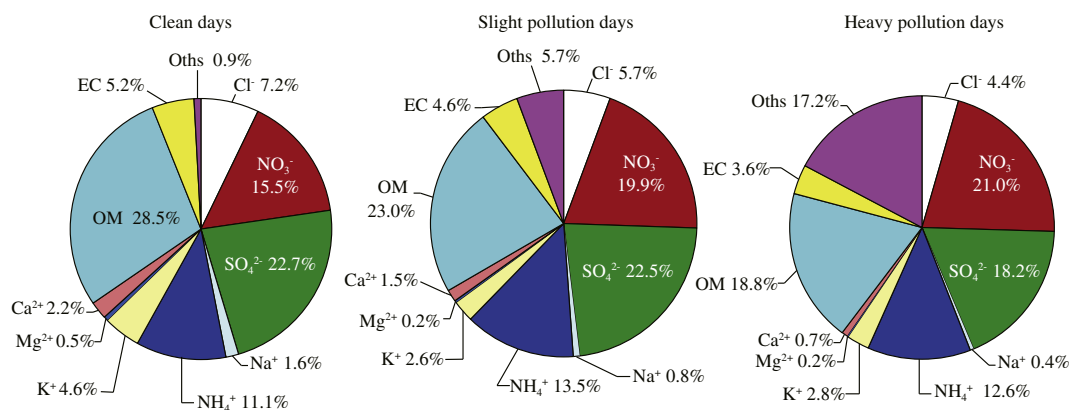


Fig. 4 – Proportions of chemical components of PM_{2.5} in clean, slight pollution and heavy pollution.

mainly through secondary reactions of gaseous pollutants like SO₂, NO_x and so on. The concentrations of SO₄²⁻ and NO₃⁻ have a close relationship with the oxidation rates of SO₂ and NO₂. Formation of SO₄²⁻ and NO₃⁻ is usually indicated by the sulfur conversion rate (SOR = $n(\text{SO}_4^{2-}) / [n(\text{SO}_4^{2-}) + n(\text{SO}_2)]$) (n refers to the molar concentration) and nitrate conversion rate (NOR = $n(\text{NO}_3^-) / [n(\text{NO}_3^-) + n(\text{NO}_2)]$) (Sun et al., 2006). The higher the values, the more the gaseous pollutants are transformed to secondary particles.

Related studies have found that the SOR is lower than 0.1 when only primary pollutants exist in the atmosphere (Truex et al., 2002; Ohta & Okita, 1990). When SOR is higher than 0.1, SO₂ in the air probably undergoes photochemical reactions (Truex et al., 2002; Ohta & Okita, 1990). Table 2 lists the SOR and NOR values calculated in 2011 in Shanghai. From the table, we can see that the annual average of SOR was 0.257, higher than 0.1, showing that photochemical reactions were quite active in Shanghai. SOR had the highest value in summer, indicating that the high temperature accelerates the gaseous reaction from SO₂ to SO₄²⁻ and the high moisture during nighttime contributed to the multi-phase SO₄²⁻ formation. By contrast, low temperature and moisture in winter led to lower sulfur conversion rates.

The annual average NOR was 0.101. The seasonal variation of NOR was a little different from that of SOR, which had lower values in summer and higher values in winter. Under high temperature conditions, the high volatility of NO₃⁻ enabled it to transfer from the particulate phase to the gaseous phase, resulting in lower NOR values in summer. However, the adverse weather conditions and high pollution emissions in

winter resulted in the frequent occurrence of haze episodes. During haze days, the NO_x emissions in Shanghai easily accumulate and form NO₃⁻ through photochemical reactions. Many research studies have proved that the NOR values during haze days are significantly higher than for non-haze days (Sun et al., 2006; Tan et al., 2009).

The ratio of [NO₃⁻]/[SO₄²⁻] is often used to indicate the relative contributions of stationary sources and mobile sources. A lower ratio means that pollution from stationary sources is more prominent than that from vehicles. Table 2 shows that the ratio of [NO₃⁻]/[SO₄²⁻] in 2011 in Shanghai was 0.943, higher than the values of 0.75, measured in 2009 in Shanghai (Huang et al., 2012), 0.71 measured in 2006 (Fu et al., 2008) and 0.43 measured in 1999 (Yao et al., 2002). This illustrates that the dramatic increase in the vehicle stock in Shanghai had a serious impact on the atmospheric environment.

2.3.2. Secondary organic carbon

Organic carbon (OC) and elemental carbon (EC) are important constituents of PM_{2.5}, contributing 20%–50% of aerosol in Chinese urban atmospheres (Lim & Turpin, 2002; Cao et al., 2007). EC is emitted directly from the incomplete combustion of fossil fuel and biomass. Because EC remains constant and does not participate in chemical reactions in the atmosphere, it is commonly used as a tracer for primary emissions (Strader et al., 1999; Castro et al., 1999). OC can consist of both primary carbon (POC) and secondary carbon (SOC); POC is mainly emitted from anthropogenic sources, and SOC is produced from atmospheric photochemical reactions of volatile organic compounds (Cabada et al., 2004).

Currently, there is no direct method to measure primary and secondary organic carbon in atmospheric aerosol. Indirect methods are often based on the EC tracer, SOA tracer (Kleindienst et al., 2007), air quality model (Lane et al., 2008), and source receptor model (Zheng et al., 2007), among which the EC tracer method (Cao et al., 2003, 2007) is the most convenient way. Since OC/EC ratios in different cities are affected by emission sources, weather conditions, instruments (different instruments may have different sensitivity to OC and EC) and so on, the estimation of SOC formation involves great uncertainty (Strader et al., 1999; Na et al., 2004). Therefore, to avoid interference from the above factors,

Table 2 – SOR, NOR values and [NO₃⁻]/[SO₄²⁻] ratios of PM_{2.5} under different seasons in 2011.

	SOR	NOR	[NO ₃ ⁻]/[SO ₄ ²⁻]
Spring	0.248	0.115	1.119
Summer	0.307	0.074	0.652
Fall	0.281	0.091	0.871
Winter	0.204	0.118	1.126
Annual	0.257	0.101	0.943

SOR: sulfate oxidizing rate; NOR: nitrate oxidizing rate.

Table 3 – Linear regression for OC and EC when OC/EC ratios were lower than $(OC/EC)_{10\%min}$ and the estimated SOC concentrations.

	$(OC/EC)_{10\%min}$	N	Linear formula	R ²	SOC	SOC/OC
Spring	2.84	202	OC = 2.43EC	0.94	3.22	35.8%
Summer	2.89	178	OC = 2.55EC	0.94	3.60	39.1%
Fall	2.78	194	OC = 2.34EC	0.93	3.42	40.4%
Winter	3.40	208	OC = 2.91EC	0.94	3.49	31.8%

OC: organic carbon; EC: elemental carbon.

researchers often use short-term OC/EC ratios to estimate SOC (Plaza et al., 2011; Yuan et al., 2006).

Following studies regarding EC as the indication of primary pollution sources, the SOC was calculated by Eq. (1) (Turpin & Huntzicker, 1995; Castro et al., 1999):

$$SOC = TOC - EC \times (OC/EC)_{pri} \quad (1)$$

where TOC represents the total organic carbon and $(OC/EC)_{pri}$ is ratio of OC/EC from primary emission sources. The assumption of this method is that there is a fixed relationship between the primary OC and EC concentrations, and the OC background concentration is constant at a given location during the season. Since $(OC/EC)_{pri}$ is highly dependent on emission sources and great difference exists in various emission sources, it is hard to define the ratio. Therefore, many studies use $(OC/EC)_{10\%min}$ (the lowest 5%–10% OC/EC ratios) measured in the environment to replace $(OC/EC)_{pri}$ (Cao et al., 2007; Yuan et al., 2006).

Considering the seasonal differences between OC and EC sources, SOC values in different seasons were estimated by $(OC/EC)_{pri}$ in corresponding seasons. Least squares regression was conducted for OC/EC values in different seasons that were lower than $(OC/EC)_{10\%min}$. Table 3 gives the regression results in the four seasons. It was found that OC and EC had a good linear correlation when the OC/EC ratio was lower than $(OC/EC)_{10\%min}$. This means that the sources of OC and EC during this period were almost the same; that is, the $(OC/EC)_{10\%min}$ value for this season can replace the $(OC/EC)_{pri}$ value.

SOC concentrations for various seasons in this research were estimated using the corresponding $(OC/EC)_{10\%min}$ values. POC

concentrations in spring, summer, fall and winter obtained in this study were 5.75, 5.61, 5.03 and 7.47 $\mu\text{g}/\text{m}^3$, respectively, and SOC concentrations in spring, summer, fall and winter obtained were 3.22, 3.60, 3.42 and 3.49 $\mu\text{g}/\text{m}^3$, respectively. The proportion of SOC in OC was 35.8%, 39.1%, 40.4% and 31.8%, respectively. SOC/OC was higher in fall and summer than in winter and spring. These values are comparable with those of Atlanta, USA (30%) (Pachon et al., 2010), Centreville, USA (36%) (Blanchard et al., 2008), California, USA (50%) (Na et al., 2004), Athens, Greece (10.1–32.5%) (Grivas et al., 2012), and Mount Heng in Hunan, China (53.9%) (Zhou et al. 2012). This implied that SOC was an important component of OC mass in Shanghai. Severe and complex air pollution often occurs during late fall and winter in Shanghai, which is caused by a stable synoptic system at the surface, decrease of the PBL height, and high relative humidity, resulting in high formation of SOC in the ambient air. In contrast, the lower temperatures and reduced sunlight in winter are not favorable for SOC formation.

2.4. Contributions of chemical components in $PM_{2.5}$ to light extinction

To investigate the contributions of individual $PM_{2.5}$ chemical components on the light extinction coefficient, Bext, the formula developed in the IMPROVE project (Interagency Monitoring of Protected Visual Environments) (Malm et al., 1994; Watson, 2002) was adopted to quantify the contributions of particles to the light extinction in Shanghai. The reconstructed Bext (Mm^{-1}) can be calculated from the mass concentrations of $PM_{2.5}$ chemical components by Eq. (2), based on the original IMPROVE algorithm (Malm et al., 1994; Watson, 2002):

$$Bext = 3f(RH)[Sulfate] + 3f(RH)[Nitrate] + 4[Organic] + 1[Soil] + 0.6[Coarse Mass] + 10[EC] + 10 \quad (2)$$

$$[Sulfate] = (NH_4)_2SO_4 \quad (3)$$

$$[Nitrate] = NH_4NO_3 \quad (4)$$

$$[Organic] = 1.4[OC] \quad (5)$$

$$[Soil] = 2.2[Al] + 2.19[Si] + 1.63[Ca] + 2.42[Fe] + 1.94[Ti] \quad (6)$$

$$[Coarse Mass] = [PM_{10}] - [PM_{2.5}] \quad (7)$$

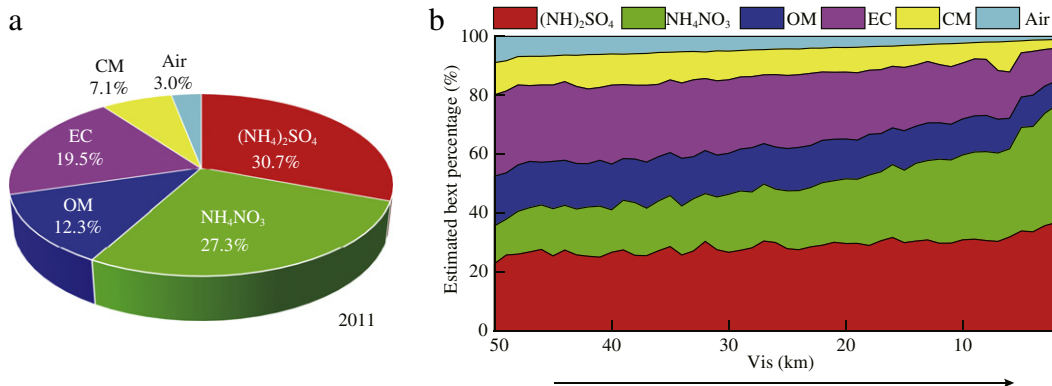


Fig. 5 – Relative contribution to light extinction of chemical components in $PM_{2.5}$ in 2011(a) and the proportions of their contributions under different visibility conditions (b).

where $f(\text{RH})$ is the hygroscopic species growth function. It indicates how scattering efficiencies increase for SO_4^{2-} and NO_3^- as they absorb liquid water (Cheung et al., 2005). The last term of the formula, the constant 10 Mm^{-1} , represents clear air scattering. We excluded the contribution of soil particles in this study since it only accounted for a small fraction of Bext (Wang, 2003). The IMPROVE formula assumes that SO_4^{2-} and NO_3^- are fully neutralized by NH_4^+ .

Fig. 5 shows the relative contribution of chemical components in $\text{PM}_{2.5}$ to light extinction in one year, and depicts the proportions of their contributions under different visibility conditions. The calculated average value of light extinction was $332.2 \pm 249.5 \text{ Mm}^{-1}$. Compared to other cities, i.e., Hong Kong (177 Mm^{-1} , Cheung et al., 2005), Jinan (292 Mm^{-1} , Yang et al., 2007), and Guangzhou ($326 \pm 248 \text{ Mm}^{-1}$, Tao et al., 2014), our result was slightly higher. $(\text{NH}_4)_2\text{SO}_4$ had the largest contribution to Bext, accounting for 30.7%; followed by NH_4NO_3 (27.3%), elemental carbon (EC) (19.5%), organic carbon (OM) (12.3%), and Coarse Mass (CM) (7.1%), as shown in Fig. 5a. The significant contribution of ammonium sulfate to visibility degradation is due to a relatively high concentration of sulfate and its ability to absorb water vapor, and a similar result was also found in other studies (Tao et al., 2009; Wang, 2003; Pui et al., 2014). In this study, we also found that there were clear differences among the contributions of chemical components with the changes in the visibility conditions, as shown in Fig. 5b. For example, under high visibility conditions, the Bext percentage of $(\text{NH}_4)_2\text{SO}_4$ was the highest, followed by EC, OM, NH_4NO_3 and CM. With the decrease of visibility, the contribution of NH_4NO_3 to Bext increased simultaneously, but the percentages of OM, EC, and CM decreased. However, the contribution from $(\text{NH}_4)_2\text{SO}_4$ was still the highest, and changed very little with the visibility degradation. The above results indicate that NH_4NO_3 and $(\text{NH}_4)_2\text{SO}_4$ were the most important chemical components responsible for visibility impairment in Shanghai.

3. Conclusions

A one-year research study on temporal variations of $\text{PM}_{2.5}$ and its chemical components, as well as their contribution to light extinction in Shanghai, were presented in this paper. The average mass concentrations of PM_{10} , $\text{PM}_{2.5}$ and $\text{PM}_{1.0}$ in 2011 were (88 ± 66), (49 ± 47) and (35 ± 30) $\mu\text{g}/\text{m}^3$, respectively. High concentrations of particulate matters occurred frequently in all seasons except summer, which is mainly because the diffusion conditions in summer are quite good and Shanghai always has rich precipitation in spring and summer. In spring and winter, NO_3^- accounted for the highest proportion in $\text{PM}_{2.5}$, while in fall and summer, SO_4^{2-} and OC had a larger proportion. In general, for all seasons in 2011 in Shanghai, secondary inorganic ions like NO_3^- , SO_4^{2-} , NH_4^+ and OM accounted for most of $\text{PM}_{2.5}$, at 75.2%–94.0% in total. This shows that both inorganic and organic pollution was serious in Shanghai. A decrease in the primary inorganic ion proportion in total components was observed with the increase of particulate mass concentration in this research. However, NO_3^- rose significantly during heavy $\text{PM}_{2.5}$ pollution days, showing that it had a close relationship with $\text{PM}_{2.5}$ pollution in Shanghai.

Photochemical reactions were quite active in Shanghai in 2011. The annual average of SOR was 0.257, much higher than 0.1. This also matches with the result that summer had higher SOR values and winter had lower SOR values. Compared with SOR, NOR had lower values in summer and higher values in winter. This is because high temperature enables NO_3^- to transfer from the particulate phase to the gaseous phase more easily. NOR can be regarded as a haze indicator since NOR values were markedly higher in haze days than in non-haze days. SOC was found to be an important component of OC mass in Shanghai, accounting for 31.8%–40.4% in 2011. High formation of SOC in the ambient air was observed during summer and fall in Shanghai. On the contrary, the lower temperatures and reduced sunlight in winter and spring were not favorable for SOC formation.

Compared with some other cities, the calculated average value of light extinction in Shanghai, (332.2 ± 249.5) Mm^{-1} , was a little higher. $(\text{NH}_4)_2\text{SO}_4$ had the largest contribution to light extinction due to the relatively high concentration of sulfate and its ability to absorb water vapor. In addition, the Bext percentage of NH_4NO_3 rose continuously with the decreasing of visibility, while the percentages of OM, EC, CM decreased. This proves that NH_4NO_3 and $(\text{NH}_4)_2\text{SO}_4$ were the major contributors to visibility impairment in Shanghai.

Acknowledgments

This work was supported by the “Chinese National Key Technology R&D Program” (No. 2014BAC22B03), the “Chinese National Non-profit Scientific Research Program” (No. 201409008), and the Key Research Project from the Science and Technology Commission of Shanghai Municipality Fund Project (No. 14DZ1202905). We also thank the anonymous reviewers for their suggestions, which helped greatly to improve the article.

REFERENCES

- Blanchard, C.L., Hidy, G.M., Tanenbaum, S., Edgerton, E., Hartsell, B., Jansen, J., 2008. Carbon in Southeastern US aerosol particles: Empirical estimates of secondary organic aerosol formation. *Atmos. Environ.* 42 (27), 6710–6720.
- Cabada, J.C., Pandis, S.N., Subramanian, R., Robinson, A.L., Polidori, A., Turpin, B., 2004. Estimating the secondary organic aerosol contribution to $\text{PM}_{2.5}$ using the EC trace method. *Aerosol Sci Technol.* 38 (S1), 140–155.
- Cao, J.J., Lee, S.C., Ho, K.F., Zhang, X.Y., Zou, S.C., Fung, K., et al., 2003. Characteristics of carbonaceous aerosol in Pearl River Delta region, China during 2001 winter period. *Atmos. Environ.* 37 (11), 1451–1460.
- Cao, J.J., Wu, F., Chow, J.C., Lee, S.C., 2005. Characterization and source apportionment of atmospheric organic and elemental carbon during fall and winter of 2003 in Xi'an, China. *Atmos. Chem. and Phys.* 5 (11), 3127–3137.
- Cao, J.J., Lee, S.C., Chow, J.C., Watson, J.G., Ho, K.F., Zhang, R.J., 2007. Spatial and seasonal distributions of carbonaceous aerosols over China. *J. Geophys. Res.* 112 (D22S11), 1–9.
- Castro, L.M., Pio, C.A., Harrison, R.M., Smith, D.J.T., 1999. Carbonaceous aerosol in urban and rural European

- atmospheres: Estimation of secondary organic carbon concentrations. *Atmos. Environ.* 33 (17), 2771–2781.
- Cheung, H.C., Wang, T., Baumann, K., Guo, H., 2005. Influence of regional pollution outflow on the concentrations of fine particulate matter and visibility in the coastal area of southern China. *Atmos. Environ.* 39 (34), 6463–6474.
- Du, H.H., Kong, L.D., Cheng, T.T., Chen, J.M., Yang, X., Zhang, R.Y., 2010. Insights into ammonium particle-to-gas conversion: Non-sulfate ammonium coupling with nitrate and chloride. *Aerosol Air Qual. Res.* 10 (6), 589–595.
- Du, H.H., Kong, L.D., Cheng, T.T., Chen, J.M., Du, J.F., Li, L., et al., 2011. Insights into summertime haze pollution events over Shanghai based on online water-soluble ionic composition of aerosols. *Atmos. Environ.* 45 (29), 5131–5137.
- Fu, Q.Y., Zhuang, G.S., Wang, J., Xu, C., Huang, K., Li, J., et al., 2008. Mechanism of formation of the heaviest pollution episode ever recorded in the Yangtze River Delta. *China. Atmos. Environ.* 42 (9), 2023–2036.
- Grivas, G., Cheristanidis, S., Chaloulakou, A., 2012. Elemental and organic carbon in the urban environment of Athens. Seasonal and diurnal variations and estimates of secondary organic carbon. *Sci. Total Environ.* 414 (1), 535–545.
- Han, T.T., Qiao, L.P., Zhou, M., Qu, Y., Du, J.F., Liu, X.G., et al., 2015. Chemical and optical properties of aerosols and their interrelationship in winter in the megacity Shanghai of China. *J. Environ. Sci.* 27, 59–69.
- Hu, M., He, L.Y., Huang, X.F., Wu, Z.J., 2009. The characteristics, sources and formation mechanisms of fine and ultrafine atmosphere particulates in Beijing. Science Press, Beijing, pp. 30–33 (in Chinese).
- Huang, K., Zhuang, G., Lin, Y., Fu, J.S., Wang, Q., Liu, T., 2012. Typical types and formation mechanisms of haze in an Eastern Asia megacity. *Shanghai. Atmos. Chem. and Phys.* 12 (1), 105–124.
- Huang, R.J., Zhang, Y.L., Bozzetti, C., Ho, K.F., Cao, J.J., Han, Y.M., et al., 2014. High secondary aerosol contribution to particulate pollution during haze events in China. *Nature* <http://dx.doi.org/10.1038/nature13774>.
- Jung, J.S., Lee, H.L., Kim, Y.J., Liu, X.G., Zhang, Y.H., Gu, J.W., et al., 2009. Aerosol chemistry and the effect of aerosol water content on visibility impairment and radiative forcing in Guangzhou during the 2006 Pearl River Delta campaign. *J. Environ. Manag.* 90 (11), 3231–3244.
- Kleindienst, T.E., Jaoui, M., Lewandowski, M., Offenberg, J.H., Lewis, C.W., Bhave, P.V., et al., 2007. Estimates of the contributions of biogenic and anthropogenic hydrocarbons to secondary organic aerosol at a southeastern US location. *Atmos. Environ.* 41 (37), 8288–8300.
- Kulkarni, S., Sobhani, N., Miller-Schulze, J.P., Shafer, M.M., Schauer, J.J., Solomon, P.A., et al., 2015. Source sector and region contributions to BC and PM_{2.5} in Central Asia. *Atmos. Chem. and Phys.* 15 (4), 1683–1705.
- Lane, T.E., Donahue, N.M., Pandis, S.N., 2008. Simulating secondary organic aerosol formation using the volatility basis-set approach in a chemical transport model. *Atmos. Environ.* 42 (32), 7439–7451.
- Li, G.L., Zhou, M., Chen, C.H., Wang, H.L., Wang, Q., Lou, S.R. et al., 2014. Characteristics of particulate matters and its chemical compositions during the dust episodes in Shanghai in Spring, 2011. *Environ. Sci.* 35(5): 1643–1653 (in Chinese).
- Li, Y.J., Lee, B.P., Su, L., Fung, J.C.H., Chan, C.K., 2015. Seasonal characteristics of fine particulate matter (PM) based on high-resolution time-of-flight aerosol mass spectrometric (HR-ToF-AMS) measurements at the HKUST supersite in Hong Kong. *Atmos. Chem. and Phys.* 15 (1), 37–53.
- Lim, H.J., Turpin, B.J., 2002. Origins of primary and secondary organic aerosol in Atlanta: Results of time-resolved measurements during the Atlanta supersite experiment. *Environ. Sci. Technol.* 36 (21), 4489–4496.
- Liu, X.G., Li, J., Qu, Y., Han, T., Hou, L., Gu, J., et al., 2013. Formation and evolution mechanism of regional haze: A case study in the megacity Beijing. *China. Atmos. Chem. and Phys.* 13 (9), 4501–4514.
- Malm, W.C., Sisler, J.F., Huffman, D., Eldred, R.A., Cahill, T.A., 1994. Spatial and seasonal trends in particle concentration and optical extinction in the United States. *J. Geophys. Res.* 99 (D1), 1347–1370.
- Moffet, R.C., Foy, B.D., Molina, M.J., Prather, K.A., 2008. Measurement of ambient aerosols in Northern Mexico City by single particle mass spectrometry. *Atmos. Chem. and Phys.* 8 (16), 4499–4516.
- Na, K., Sawant, A.A., Song, C., Cocker, D.R., 2004. Primary and secondary carbonaceous species in the atmosphere of Western Riverside Country. California. *Atmos. Environ.* 38 (9), 1345–1355.
- Ohta, S., Okita, T., 1990. A chemical characterization of atmospheric aerosol in Sapporo. *Atmos. Environ.* 24 (4), 815–822.
- Pachon, J.E., Balachandran, S., Hu, Y.T., Weber, R.J., Mulholland, J.A., Russel, A.G., 2010. Comparison of SOC estimates and uncertainties from aerosol chemical composition and gas phase data in Atlanta. *Atmos. Environ.* 44 (32), 3907–3914.
- Park, S.S., Hong, S.B., Jung, Y.G., Lee, J.H., 2004. Measurement of PM₁₀ aerosol and gas-phase nitrous acid during fall season in a semi-urban atmosphere. *Atmos. Environ.* 38 (2), 293–304.
- Pateraki, S., Asimakopoulos, D.N., Bougiatioti, A., Maggos, T., Vasilakos, C., Mihalopoulos, N., 2014. Assessment of PM_{2.5} and PM₁ chemical profile in a multiple-impacted Mediterranean urban area: Origin, sources and meteorological dependence. *Sci. Total Environ.* 479–480, 210–220.
- Plaza, J., Artano, B., Salvador, P., Gomez-Moreno, F.J., Pujadas, M., Pio, C.S., 2011. Short-term secondary organic carbon estimations with a modified OC/EC primary ratio method at a suburban site in Madrid (Spain). *Atmos. Environ.* 45 (15), 2496–2506.
- Pui, D.Y.H., Chen, S.C., Zuo, Z.L., 2014. PM_{2.5} in China: measurements, sources, visibility and health effects, and mitigation. *Particuology.* 13 (2), 1–26.
- Qiao, L.P., Cai, J., Wang, H.L., Wang, W.B., Zhou, M., Lou, S.R., et al., 2014. PM_{2.5} constituents and hospital emergency-room visits in Shanghai, China. *Environ. Sci. Technol.* 48 (17), 10406–10414.
- Quan, J.N., Tie, X.X., Zhang, Q., Liu, Q., Li, X., Gao, Y., et al., 2014. Characteristics of heavy aerosol pollution during the 2012–2013 winter in Beijing. *China. Atmos. Environ.* 88 (5), 83–89.
- Safai, P.D., Budhavant, K.B., Rao, P.S.P., Ali, K., Sinha, A., 2010. Source characterization for aerosol constituents and changing roles of calcium and ammonium aerosols in the neutralization of aerosol acidity at a semi-urban site in SW India. *Atmos. Res.* 98 (1), 78–88.
- Seinfeld, J.H., Pandis, S.N., 2006. *Atmospheric chemistry and physics: From air pollution to climate change.* Wiley, New York, p. 213.
- Sokolik, I.N. and Toon, O.B. 1996. Direct radiative forcing by anthropogenic airborne mineral aerosols. *J. Aerosol. Sci.* 27(Supplement 1): 11–12.
- Strader, R., Lurmann, F., Pandis, S.N., 1999. Evaluation of secondary organic aerosol formation in winter. *Atmos. Environ.* 33 (29), 4849–4863.
- Sun, K., Qu, Y., Wu, Q., Han, T.T., Gu, J.W., Zhao, J.J., et al., 2014. Chemical characteristics of size-resolved aerosols in winter in Beijing. *Sci. Total Environ.* 26 (8), 1641–1650.
- Sun, Y.L., Zhang, G.S., Tang, A.H., Wang, Y., An, Z.S., 2006. Chemical characteristics of PM_{2.5} and PM₁₀ in haze-fog episodes in Beijing. *Environ. Sci Technol.* 40 (10), 3148–3155.
- Tan, J.H., Duan, J.C., Chen, D.H., Wang, X.H., Guo, S.J., Bi, X.H., et al., 2009. Chemical characteristics of haze during summer and winter in Guangzhou. *Atmos. Res.* 94 (2), 238–245.
- Tang, X.Y., Zhang, Y.H., Shao, M., 2006. *Atmospheric environmental chemistry (2nd edition).* Higher Education Press, Beijing, pp. 175–180 (in Chinese).

- Tao, J., Ho, K.F., Chen, L.G., Zhu, L.H., Han, J.L., Xu, Z.C., 2009. Effect of chemical composition of PM_{2.5} on visibility in Guangzhou, China, 2007 spring. *Particuology*. 7 (1), 68–75.
- Tao, J., Zhang, L.M., Ho, K.F., Zhang, R.J., Lin, Z.J., Zhang, Z.S., et al., 2014. Impact of PM_{2.5} chemical compositions on aerosol light scattering in Guangzhou — The largest megacity in South China. *Atmos. Res.* 135–136 (1), 48–58.
- Truex, T.J., Pierson, W.R., McKee, D.E., 2002. Sulfate in diesel exhaust. *Environ. Sci. Technol.* 14 (9), 1118–1121.
- Turpin, B.J., Huntzicker, J.J., 1995. Identification of secondary organic aerosol episodes and quantitation of primary and secondary organic aerosol concentrations during SCAQS. *Atmos. Environ.* 29 (23), 3527–3544.
- Turpin, L., Turpin, B.J., Lim, H.J., 2001. Species contributions to PM_{2.5} mass concentrations: Revisiting common assumption for estimating organic mass, *aerosol Sci. Technol.* 35 (1), 602–610.
- Wang, T., 2003. Study of visibility and its causes in Hong Kong. Final report to the environmental protection department of Hong Kong, Hong Kong.
- Wang, T., Jiang, J.F., Deng, J.J., Shen, Y., Fu, Q.Y., Wang, Q., et al., 2012. Urban air quality and regional haze weather forecast for Yangtze River Delta region, *Atmos. Environ.* 58 (15), 70–83.
- Wang, Y., Zhuang, G.S., Sun, Y.L., An, Z.S., 2005. Water-soluble part of the aerosol in the dust storm season—Evidence of the mixing between mineral and pollution aerosols. *Atmos. Environ.* 39 (37), 7020–7029.
- Wang, Y., Zhuang, G.S., Zhang, X.Y., Huang, K., Xu, C., Tang, A.H., et al., 2006a. The ion chemistry, seasonal cycle, and sources of PM_{2.5} and TSP aerosol in Shanghai. *Atmos. Environ.* 40 (16), 2935–2952.
- Wang, Y., Zhuang, G.S., Zhang, X.Y., An, S.Z., 2006b. The variation of characteristics and formation mechanisms of aerosols in dust, haze, and clear days in Beijing. *Atmos. Environ.* 40 (34), 6579–6591.
- Watson, J.G., 2002. Critical review-visibility: Science and regulation. *J. Air Waste Manage. Assoc.* 52, 628–713.
- Yang, L.X., Wang, D.C., Cheng, S.H., Wang, Z., Zhou, Y., Zhou, X.H., et al., 2007. Influence of meteorological conditions and particulate matter on visual range impairment in Jinan. *China. Sci. Total Environ.* 383 (1–3), 164–173.
- Yao, X.H., Chan, C.K., Fang, M., Cadle, S., Chan, T., Mulawa, P., et al., 2002. The water-soluble ionic composition of PM_{2.5} in Shanghai and Beijing, China. *Atmos Environ.* 36 (26), 4223–4234.
- Ye, B.M., Ji, X.L., Yang, H.Z., Yao, X.H., Chan, C.K., Cadle, S.H., et al., 2003. Concentration and chemical composition of PM_{2.5} in Shanghai for a 1-year period. *Atmos Environ* 37 (4), 499–510.
- Yuan, Z.B., Yu, J.Z., Lau, A.K.H., Louie, P.K.K., Fung, J.C.H., 2006. Application of positive matrix factorization in estimating aerosol secondary organic carbon in Hong Kong and its relationship with secondary sulfate. *Atmos. Chem. and Phys.* 6 (1), 25–34.
- Zhang, R., Jing, J., Tao, J., Hsu, S.C., Wang, G., Gao, J., et al., 2013. Chemical characterization and source apportionment of PM_{2.5} in Beijing: Seasonal perspective. *Atmos. Chem. and Phys.* 13 (14), 7053–7074.
- Zheng, M., Cass, G.R., Ke, L., Wang, F., Schauer, J.J., Edgerton, E.S., et al., 2007. Source apportionment of daily fine particulate matter at Jefferson Street, Atlanta, GA, during summer and winter. *J. Air Waste Manage. Assoc.* 57 (2), 228–242.
- Zhou, S.Z., Wang, Z., Gao, R., Xue, L.K., Yuan, C., Wang, T., et al., 2012. Formation of secondary organic carbon and long-range transport of carbonaceous aerosols at Mount Heng in South China. *Atmos. Environ.* 63 (15), 203–212.